

A.2 Suprathermal Electron Telescope (STE)

Version: 2021-05-13

A.2.1 Overview

The Suprathermal Electron (STE) instrument, part of the IMPACT investigation on both spacecraft of NASA's STEREO mission, is designed to measure electrons from ~ 2 to ~ 100 keV. This is the primary energy range for impulsive electron/ ^3He -rich energetic particle events that are the most frequently occurring transient particle emissions from the Sun, for the electrons that generate solar type III radio emission, for the shock accelerated electrons that produce type II radio emission, and for the superhalo electrons (whose origin is unknown) that are present in the interplanetary medium even during the quietest times. These electrons are ideal for tracing heliospheric magnetic field lines back to their source regions on the Sun and for determining field line lengths, thus probing the structure of interplanetary coronal mass ejections (ICMEs) and of the ambient inner heliosphere. STE utilizes arrays of small, passively cooled thin window silicon semiconductor detectors, coupled to pulse-reset front-end electronics, to detect electrons down to ~ 2 keV with about 2 orders of magnitude increase in sensitivity over previous sensors at energies below ~ 20 keV. STE provides energy resolution of $E/E \sim 10\text{--}25\%$ and the angular resolution of $\sim 20^\circ$ over two oppositely directed $\sim 80^\circ \times 80^\circ$ fields of view centered on the nominal Parker spiral field direction (45° from the spacecraft-Sun line for STE-U, 225° for STE-D) when the spacecraft is in its nominal orientation. These detectors and their associated angle bins are stationary with respect to the spacecraft, therefore when the spacecraft is rolled 180° as it is after Solar Conjunction (i.e. after July 2015). Therefore, STE-U is centered 315° from the spacecraft-Sun line and STE-D 135° in the post-Solar Conjunction orientation.

A.2.1.1 Heritage

STE is a unique instrument designed to provide geometry factor times observing time product about two orders of magnitude larger than previous detectors (electrostatic analyzers) in the ~ 2 to 20 keV energy range, with much lower background. Electrostatic analyzers such as the very large EESA-H sensor (~ 20 cm diam, ~ 3 kg, ~ 3 W) of the 3D Plasma & Energetic Particle instrument (Lin et al. 1995) on the Wind spacecraft measure one energy band at a time. EESA-H has $E/E = \sim 0.2$ so ~ 14 contiguous energy steps covered 2–20 keV, a duty cycle of $\sim 7\%$ at a given energy. STE utilizes passively cooled silicon semiconductor detectors (SSDs) that measure all energies simultaneously (100% duty cycle). Prior to STE the SSDs used for particle detection have had relatively high capacitance and leakage currents, resulting in electronic noise thresholds of $> \sim 15$ keV, and thick window dead layers that further increase the minimum energy detectable to $\sim 20\text{--}30$ keV for electrons and ions.

A.2.1.2 Product Description

STE covers electrons in the energy range $\sim 2\text{--}20$ keV which are present as a superhalo on the solar wind electrons, and as CME shock-accelerated, or flare-accelerated populations extending beyond the IMPACT SWEA range. STE consists of arrays of small, low capacitance, cooled SSDs, fabricated with an unusually thin window dead layer (Tindall et al. 2008), so $< \sim 2$ keV electrons can penetrate and be detected. The SSDs are surrounded by a guard ring and passively cooled to ~ -30 to -90°C to minimize leakage current, and

coupled to cooled FET, pulse-reset preamp-shaping electronics to obtain an electronic threshold of ~ 1.5 keV. STE's silicon semiconductor devices (SSDs) measure all energies simultaneously. The STE consists of two arrays of four SSDs in a row, each ~ 0.1 cm² area and ~ 500 microns thick. Each array looks through a rectangular opening that provides a $\sim 20 \times 80$ degree field of view for each SSD with the 80 degree direction perpendicular to the ecliptic. Adjacent FOVs are offset for a total FOV of $\sim 80 \times 80$ degrees. The two arrays are mounted back-to-back, looking in opposite directions, centered about 25 deg. from the average Parker Spiral field direction. The two arrays were designated STE-U (upstream) for the more sunward-looking unit and STE-D (downstream) for the unit sensitive to electrons directed toward the Sun. STE is located just inboard of SWEA on the STEREO boom to clear its field of view and remain in shadow. Details of STE's design can be found in the instrument review paper by Lin et al. (2008).

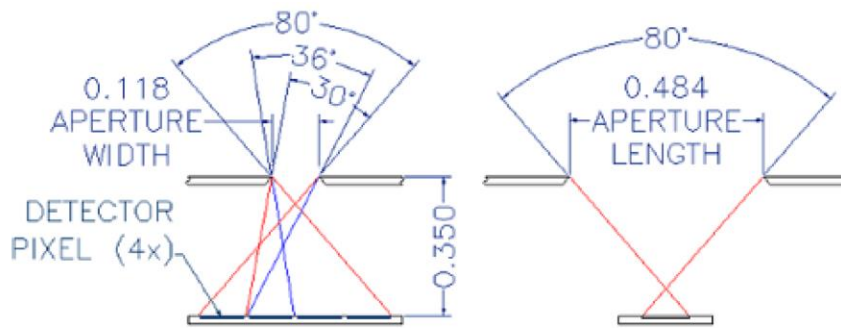


Figure 1 Schematic of FOV for STE-D (Lin et al., 2008)

Spectra packets contain the accumulated spectra data. Each energy bin count is log-compressed to 8-bits. In normal mode, a Spectra packet contains all the accumulated spectra for STE-U and STE-D (32 energies time 4 detectors times two STE units = 256 counters per spectra packet). During commissioning, it was found that the STE-U detectors were saturated by reflected sunlight rendering the data from STE-U unusable. STE-U data were removed from the spectra packets on 2009-04-16 on both STEREO spacecraft. The usable archived STE data are thus only from STE-D.

A.2.2 Theoretical Description

STE distribution data are transmitted from the spacecraft in log-compressed counts. The exact format of the STE data packets and the log compression are given in the IMPACT Command and Telemetry Database: http://sprg.ssl.berkeley.edu/impact/peters/IMPACT_CTM.xls

These data can be converted into physical units, specifically flux, using the following methodology. All code below is in IDL, and the full code is given just after this explanation.

The formula for conversion from counts to flux is this:

$$\text{flux} = \text{cnt} / (\text{dt} * \text{gf} * \text{denenergy})$$

where:

cnt is the STE data in counts

dt is the time over which counts were collected for each data point, nominally 10s

gf is the geometric factor in $\text{cm}^2 \cdot \text{steradians}$. For STE-D the value is 0.029 for detectors 0 and 1, and 0.021 for detectors 2 and 3.

denenergy is the width of each energy bin in eV.

The energy bins of the instrument are given in the following table.

Table Nominal STE Energy Bins. The energy bins accumulate events from the next energy level below to the energy level indicated; bin "0" counts from the discriminator threshold level to the indicated level

Bin	Energy, keV	Bin	Energy, keV	Bin	Energy, keV	Bin	Energy
0	2.00	8	6.00	16	11.21	24	26.99
1	2.50	9	6.50	17	12.27	25	31.14
2	3.00	10	7.00	18	13.50	26	36.32
3	3.50	11	7.50	19	14.92	27	42.92
4	4.00	12	8.08	20	16.58	28	51.49
5	4.50	13	8.72	21	18.53	29	62.91
6	5.00	14	9.45	22	20.84	30	78.60
7	5.50	15	10.27	23	23.62	31	100.0

What follows is the code used to calculate electron flux from the STE Level 1 data. This code is written in IDL and relies on the SPEDAS library

```
;  
;+  
;PROCEDURE:      ste_cnt_to_flux  
;PURPOSE:  
;  Convert count to flux, for STE data  
;  
;INPUTS:  
;  name: tplot variable from load_sta_l1_ste, etc.  
;KEYWORDS:  
;  sum_bin:  what bins to sum over for energy bands, ~intarr[32]  
;            e.g. [-1,0,0,0,1,1,1,1,.....] , then bin# 1,2,3 for band  
#0;  
;            bin# 4,5,6 for band #1.  
; gm_factor: geometric factors  
;  df : if set, get distribution function  
;  delta_t : if set, average the data due to delta_t ( in seconds)  
;  p : if set, the flux and df is converted for protons  
;  U ; if set, convert the flux for STE-U detectors  
;OUTPUTS:  
;  ee : central energy of energy band
```

```

; e0,e1: lower and upper bound of energy band
;
;CREATED BY:      Linghua Wang
;LAST MODIFIED:  02/27/09
;
;-

pro ste_cnt_to_flux,name,sum_bin = sum_bin,gm_factor =
gm_factor,ee=ee,e0=e0,e1=e1, df = df, delta_t = delta_t, p = p, U= U

nn = n_elements(name)

if not keyword_set (p) then mass =9.1094d-31 else mass = 1.67262d-27
; in kilogram for electrons or protons

if not keyword_set(sum_bin) then sum_bin = indgen(32)

if not keyword_set(gm_factor) then begin
;gm_factor = replicate(0.43*0.1,nn) ; old rough gf in cm^2 * str
for STE one pixel
if not keyword_set(U) then begin
gm_factor = [0.029,0.029,0.021,0.021] ; for STE-D
print,'STE-D'
endif else begin
gm_factor = [0.022,0.022,0.0173,0.0173] ; for STE-U
print,'STE-U'
endelse
endif else begin
if n_elements(gm_factor) eq 1 then gm_factor =
replicate(gm_factor,nn)
endelse

emin = 1.5d3 ; in eV, the lowest energy for bin #0, could be
incorrect

n_e = max(sum_bin)

ee = fltarr(n_e+1,nn)
e0 = fltarr(n_e+1,nn)
e1 = fltarr(n_e+1,nn)

for i =0, nn-1 do begin
get_data, name(i),data=pp,dl=dl
yy = pp.y
vv = pp.v* 1.e3 ; in eV
xx = pp.x
nt2 = n_elements(xx)

if keyword_set(delta_t) then begin
ni = -1
nt = 0

```

```

xx2 = dblarr(nt2)
yy2 = fltarr(nt2,32)
vv2 = fltarr(nt2,32)
dtt0 = dblarr(nt2)

while(ni lt nt2 - 1) do begin
  tt0 = xx(ni+1)
  tlist = where((xx lt tt0 + delta_t) and (xx ge tt0 - 1.e-6),
tind)
  if tind gt 0L then begin
    xx2(nt) = average(xx(tlist),/nan)
    yy2(nt,0:31) = total(yy(tlist,*),1,/nan)
    vv2(nt,0:31) = average(vv(tlist,*),1,/nan)
    dtt0(nt) = tind*10.d0 ;; original time resolution is 10 s
    nt = nt+1
    ni = tlist(tind-1)

  endif
endwhile

xx = xx2(0:nt-1)
yy = yy2(0:nt-1,*)
vv = vv2(0:nt-1,*)
tt = dtt0(0:nt-1)
endif else begin
  nt = nt2
  tt = 10.d0
endelse

dt = fltarr(nt,n_e+1)
denergy = fltarr(nt,n_e+1)
cnt = fltarr(nt,n_e+1)
e_min = fltarr(nt,32)
e_max = fltarr(nt,32)
old_e = fltarr(nt,n_e+1)
cent_e = fltarr(nt,n_e +1)
low_e = fltarr(nt,n_e+1)
up_e = fltarr(nt,n_e+1)

gf = replicate(gm_factor(i),nt,n_e+1)

e_max = vv
e_min(*,1:31) = vv(*,0:30)
e_min(*,0) = replicate(emin,nt)

for j =0, n_e do begin
  dt(*,j) = tt
  elist = where(sum_bin eq j, eind)
  if eind eq 1 then begin
    cnt(*,j) = yy(*,elist)

```

```

    denergy(*,j) = e_max(*,elist) - e_min(*,elist)
    old_e(*,j) = vv(*,elist)
    cent_e(*,j) = (e_max(*,elist) + e_min(*,elist))/2.0
    low_e(*,j) = e_min(*,elist)
    up_e(*,j) = e_max(*,elist)
endif else begin
    cnt(*,j) = total(yy(*,elist),2,/nan)
    denergy(*,j) = e_max(*,elist(eind-1)) - e_min(*,elist(0))
    old_e(*,j) = average(vv(*,elist), 2, /nan)
    cent_e(*,j) = (e_max(*,elist(eind-1)) + e_min(*,elist(0)))/2.0
    low_e(*,j) = e_min(*,elist(0))
    up_e(*,j) = e_max(*,elist(eind-1))
endelse

endfor

; correct for the energy loss

if keyword_set(p) then begin
    denergy = denergy *1.06538
    cent_e = cent_e*1.06538 + 2.3e3
    old_e = old_e*1.06538 + 2.3e3
    low_e = low_e*1.06538 + 2.3e3
    up_e = up_e*1.06538 + 2.3e3
endif else begin
    cent_e = cent_e + 350.
    old_e = old_e + 350.
    low_e = low_e + 350.
    up_e = up_e + 350.
endelse

flux = cnt/(dt * gf * denergy)

store_data, name(i)+'_f', data = {x:xx, y:flux, v:
cent_e,v2:old_e}, dl=dl
options,name(i)+'_f','spec',0

options,name(i)+'_f','labels',strmid(strtrim(average(cent_e,1,/nan)/1.
e3,2),0,4) + 'keV'
options,name(i)+'_f','colors',[1,2,3,4,5,6]

ee(*,i) = average(cent_e,1,/nan)
e0(*,i) = average(low_e,1,/nan)
e1(*,i) = average(up_e,1,/nan)

if keyword_set(df) then begin
    if keyword_set(p) then begin

        vel = velocity_new(cent_e,/p) * 1.d0 ; m/s, velocity for
proton
        gamma = cent_e/938.27d6 + 1.

```

```

        d_f = cnt/(dt * gf * 1.d-4 * denenergy *1.602d-19 * vel * vel /
(mass * gamma * gamma * gamma))
        store_data, name(i)+'_df', data = {x:xx, y:d_f, v:
cent_e,v2:old_e}, dl=dl
        options,name(i)+'_df','spec',0

options,name(i)+'_df','labels',strmid(strtrim(average(cent_e,1,/nan)/1
.e3,2),0,4) + 'keV'
        options,name(i)+'_df','colors',[1,2,3,4,5,6]
endif else begin

        vel = velocity_new(cent_e,/e) * 1.d0 ; m/s
        gamma = cent_e/0.511d6 + 1.
        d_f = cnt/(dt * gf * 1.d-4 * denenergy *1.602d-19 * vel * vel /
(mass * gamma * gamma * gamma))
        store_data, name(i)+'_df', data = {x:xx, y:d_f, v:
cent_e,v2:old_e}, dl=dl
        options,name(i)+'_df','spec',0

options,name(i)+'_df','labels',strmid(strtrim(average(cent_e,1,/nan)/1
.e3,2),0,4) + 'keV'
        options,name(i)+'_df','colors',[1,2,3,4,5,6]
endelse

endif

endifor

return

end

```

A.2.3 Forward Model (if applicable)

NOTE: Not applicable to STE.

A.2.4 Inverse Model (if applicable)

NOTE: Not applicable.

A.2.5 Error Analysis and Corrections

The STE detectors see some contamination from the radioactive source in the door when the door is open. Such contamination appears to be strongest in D3 and affects the data mainly around 20-25 keV with a weak count rate of < 0.03 /s. It only shows up when the solar wind suprathermal electron intensity is very low at those energies. We used the STE configurations to simulate the contamination from the door source when the door is open, but the results produced a smaller effect than the observed contamination. However our test established that such contamination only shows up when the solar wind suprathermal electron intensity is very low.

On the other hand, there is large noise in the #28th-29th energy channels (if the channel number starts from #0) in D0 on the STEREO A and in the #26th-27th energy channels in D0 on the STEREO B, probably due to some electronic noise. It is suggested that users ignore the observations in these energy channels of D0 when they analyze the data for scientific research. There is also some large noise in the first 3 or 4 energy channels in D2, probably also due to some electronic noise. Figure 2 demonstrates this noise issue.

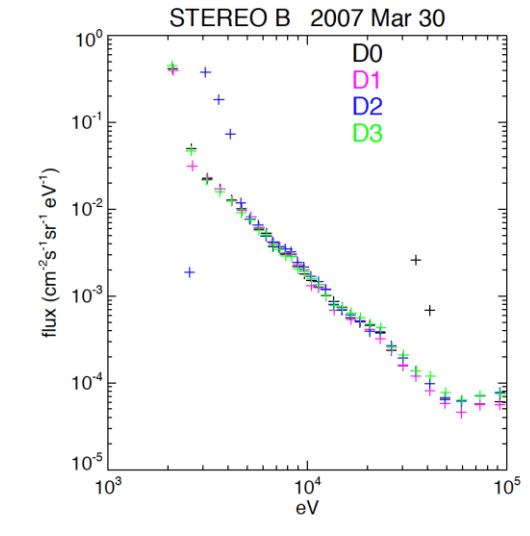


Figure 2: The observed flux in STE-D0,D1,D2,D3 on STEREO B on March 30, 2007

A.2.6 Calibration and Validation

A.2.6.1 Calibration

1.1.1.1. Pre-flight/On-ground Calibration

Calibrations of the STE instruments were performed in the laboratory using radioactive sources and an electron gun. Figure 3 shows a typical spectrum for a STE detector exposed to ^{55}Fe and ^{109}Cd radioactive sources simultaneously, taken at room temperature. The ^{55}Mn $K\alpha$ X-ray at 5.9 keV is the largest peak in the spectrum and the 3 keV peak from the daughter isotope ^{109}Ag is clearly evident. The broad peaks centered around 68 keV and 40 keV are due to the 84 and 62 keV ^{109}Cd conversion electrons that have lost energy in the source and detector Windows. A similar $^{109}\text{Cd}/^{55}\text{Fe}$ radioactive source on the inside of the STE recloseable door provides in-orbit calibration of the SSDs.

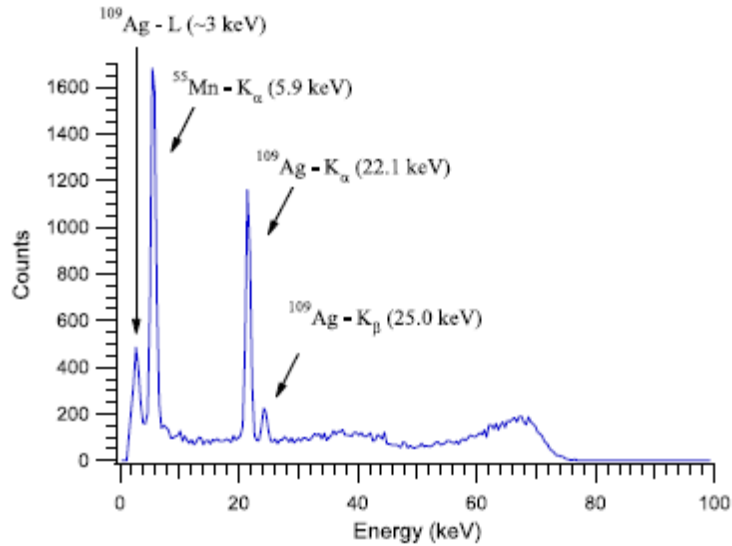


Figure 3: Spectrum obtained by illuminating a STE detector at ambient temperature with a source of one μCi ^{55}Fe and a one μCi ^{109}Cd simultaneously. The integration time is not sufficient to show the 88 keV gamma emission of the ^{109}Cd . The broad peaks centered around 68 keV and 40 keV are due to the 84 and 62 keV ^{109}Cd conversion electrons that have lost energy in the source and detector Windows. A combination of ^{109}Cd and ^{55}Fe radioactive source to the inside of the door provides in-orbit calibration of the SSDs when door is closed

The primary calibration involved measuring the response of the STE SSDs to incident electrons of known energy from an accelerator. Photo-electrons generated by a UV lamp illuminating a specially coated photo-anode accelerated through a potential drop produce a wide (~3 cm) parallel mono-energetic electron beam with energy adjustable from 0 to 30 keV. A Helmholtz coil was positioned outside the chamber to nullify the Earth's magnetic field and minimize the curvature of low energy electrons.

In addition, an on-board Test Pulser that runs at ~2000 c/s with a ramping amplitude, cycling every 40 seconds, is used to stimulate the preamplifier and downstream electronics chain and verify the stability and linearity of the electronics. The tests used two modes; smoothly ramping (good for testing ADC DNL), and stepping over 8 linearly spaced discrete amplitudes (for calibrating front end gain and electronic noise).

The left-hand panel of Figure 4 shows the pulse height distribution of one SSD in the STE instrument for normally incident 4 keV electrons. The largest peak is observed with center energy at the STE ADC channel 18.4, along with an overlying Gaussian fit showing a FWHM of 1.1 keV. The low energy excess below the peak is due to the roughly 5 to 10% of electrons incident upon the SSD that scatter back out of the detector, resulting in partial energy deposition.

The STE sensor was mounted on a 3-axis manipulator to allow the instrument response to be determined as a function of the 2 incident angles and linear position

along to the beam width. Figure 5 shows the total count rate observed in each of the four pixels of STE-U as a function of the azimuth angle. This measurement was performed while keeping the electron beam energy constant at 10 keV.

For comparison, in Figure 6, left panel, shows observations of an impulsive solar electron event, and in the right panel, the energy spectra for both the pre-event background and for the peak flux at each energy for the event, from STE-D from the B spacecraft. The lowest energy point is at 2 keV, and shows some detector noise as expected. This is an active time when the pre-event background is dominated by solar electron fluxes.

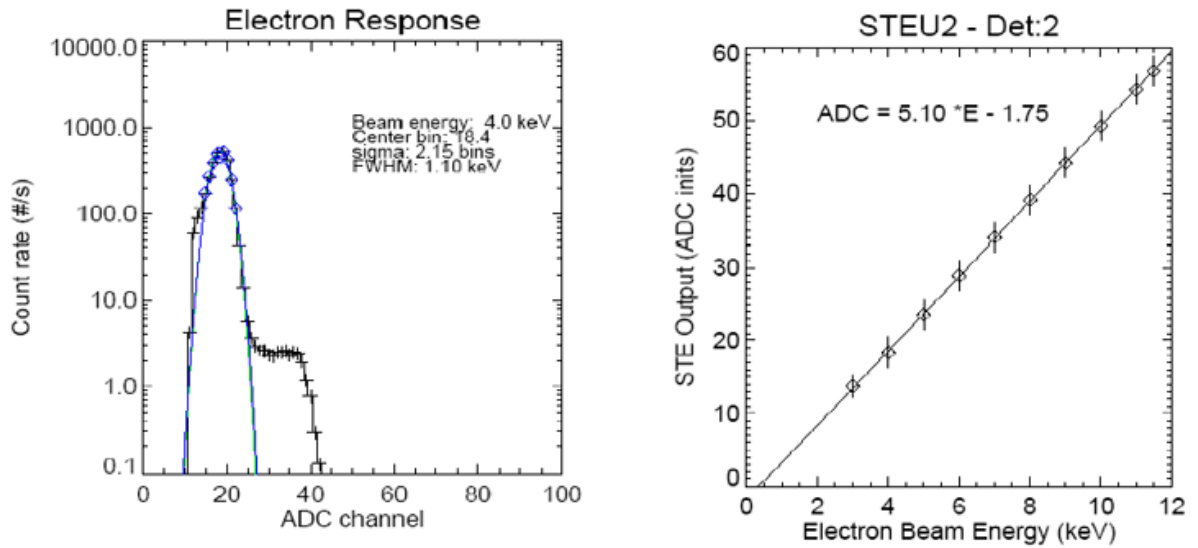


Figure 4: Left panel: Response of a STE detector to a normally incident beam of 4 keV electrons. The fit to the peak gives ~ 1.1 keV FWHM energy resolution. The secondary peak at twice the energy is due to pulse pileup from two electrons striking the detector simultaneously, unusually prominent because the beam is pulsed. Right panel: STE ADC channel output for different energy electrons (vertical error bars dominated by FWHM width of the detector response)

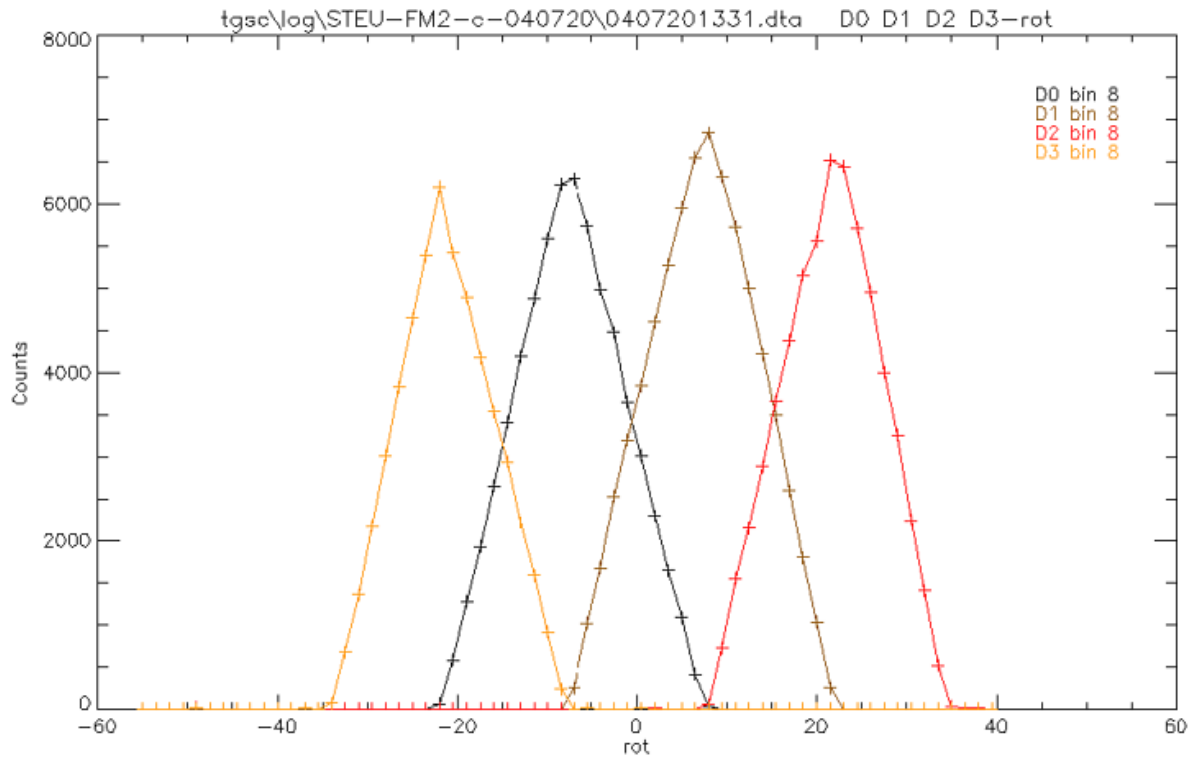


Figure 5: Angular response in azimuth angle (0° is normal incident to the detector plane) for the four detectors of the STE-U sensor

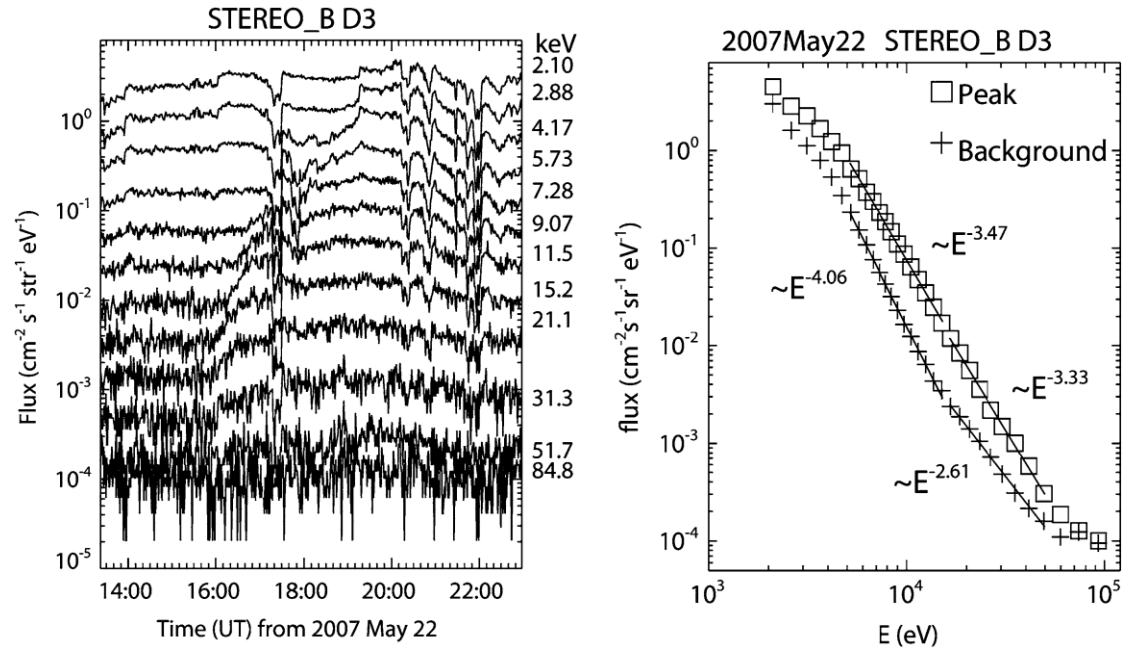


Figure 6: Left panel: One-minute average electron fluxes observed downstream by a single STE detector on 2007 May 22. A solar energetic electron event begins at ~ 1555 UT, with velocity dispersion evident down to ~ 3 keV. Right panel: Energy spectra from the same detector. The squares indicate the peak fluxes observed in the 32 energy bins, and the crosses show the pre-event electron fluxes

1.1.1.2. In-flight Calibration

A radioactive source is embedded in the STE door. This source is used to calibrate the instrument in flight. For the in-flight calibrations, we compared the observed counts with the estimates based on the ground calibration. They agree with each other as seen in Figure 7.

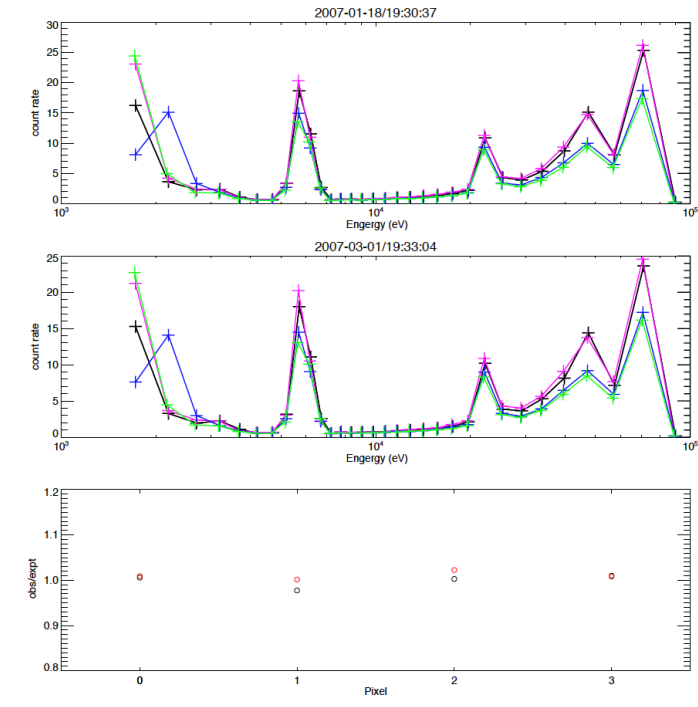


Figure 7 showing the observed count rate in STE-D1 on STEREO A during two in-flight calibration periods and the count ratio in four detector pixels.

A.2.6.2 Validation

The flight-calibration data was used to validate the STE measurements. When STEREO was close to the Earth, data from the WIND/3DP instrument was used to cross-calibrate the STE data. The STE data agreed well with WIND/3DP electron data as seen in Figure 8.

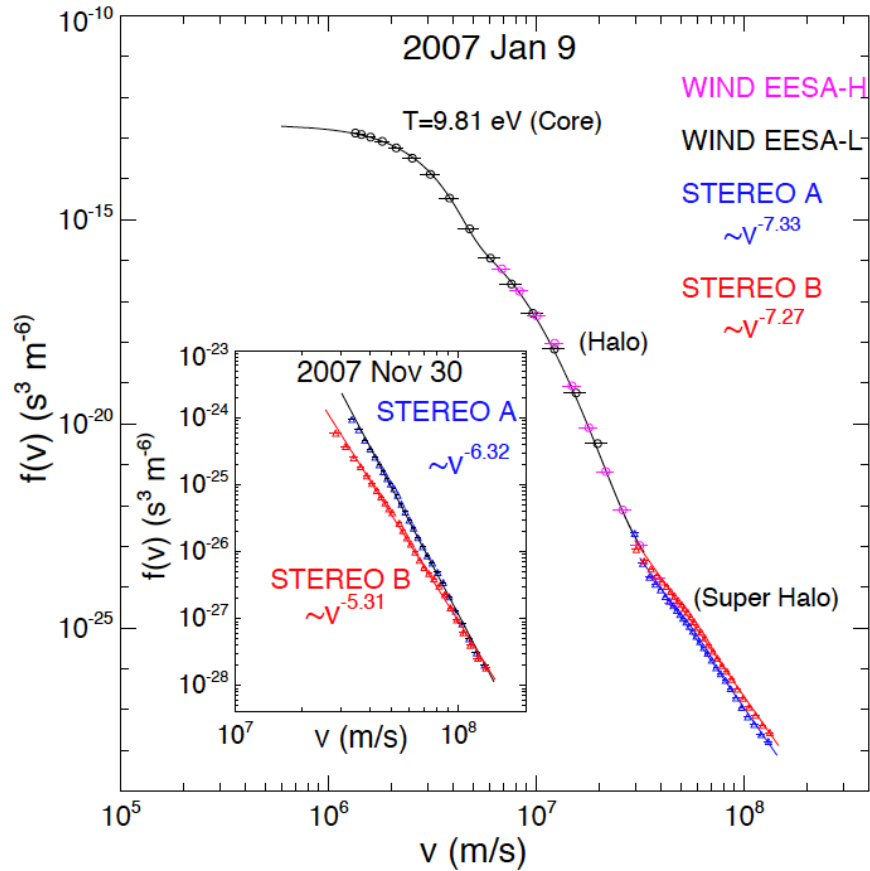


Figure 8: Omnidirectional electron differential flux spectrum from 5eV to 100keV measured at a very quiet time on 9 January 2007 by the WIND and twin STEREO spacecraft in close vicinity to the Earth. Taken from Yoon et al. (2012)

A.2.7 References

Lin, R.P., Curtis, D.W., Larson, D.E. et al. The STEREO IMPACT Suprathermal Electron (STE) Instrument. *Space Sci Rev* 136, 241–255 (2008). <https://doi.org/10.1007/s11214-008-9330-7>.

Yoon, PH; Ziebell, LF; Gaelzer, R; Lin, RP; Wang, L, Langmuir turbulence and suprathermal electrons, *Space Science Reviews*, 173(1-4), 459-489, 2012